

### Supplementary material

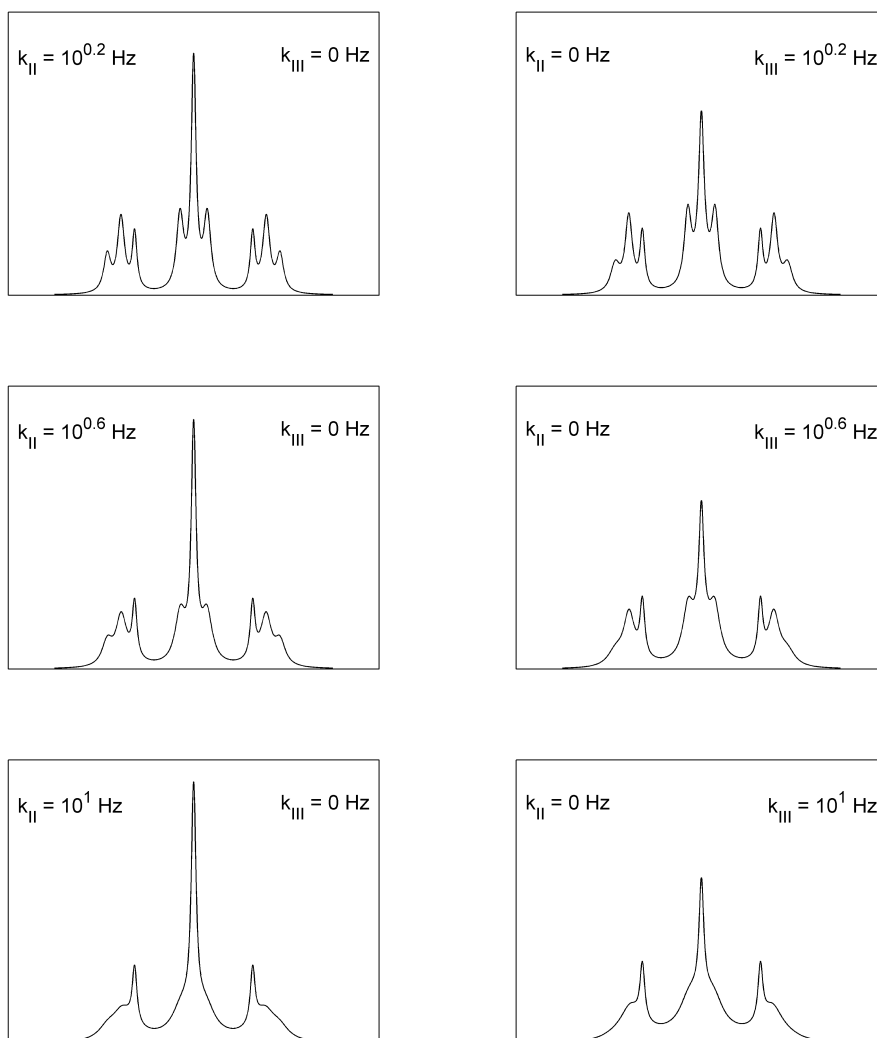


Figure S1. Effect of  $k_{II}$  and of  $k_{III}$  on the dynamical NMR lineshape computed for the 4-site exchange model.  $k_{II}$  is related to simultaneous *cis-trans* exchange in both diphosphine ligands, whereas  $k_{III}$  is related to *cis-trans* exchange in a single diphosphine ligand.

The NMR dynamical lineshape under reaction types II and III differ in the behaviour of the central line. Under simultaneous *cis-trans* exchange in both diphosphine ligands (type II) the central line remains narrow even in the coalescence region, whereas it broadens significantly under *cis-trans* exchange in a single ligand (type III). [The line

broadening is best (though somewhat indirectly) observed as line amplitude decreasing.] This behaviour is easily explained by reference to Figure 1. Consider the  $^{31}\text{P}$  spin configurations contributing to the central line and, in particular, the  $\alpha\beta\beta\alpha$  and  $\beta\alpha\alpha\beta$  configurations that are affected by the dynamics within the 4-site model. Under double exchange these are transformed into each other and do not undergo line broadening because the dynamics does not affect their frequency. Conversely, single exchange transforms the  $\alpha\beta\beta\alpha$  and  $\beta\alpha\alpha\beta$  configurations into  $\beta\beta\alpha\alpha/\alpha\alpha\beta\beta$  and  $\alpha\alpha\beta\beta/\beta\beta\alpha\alpha$ , respectively, thus shifting their resonant frequency and causing dynamical broadening.

### Supplementary material

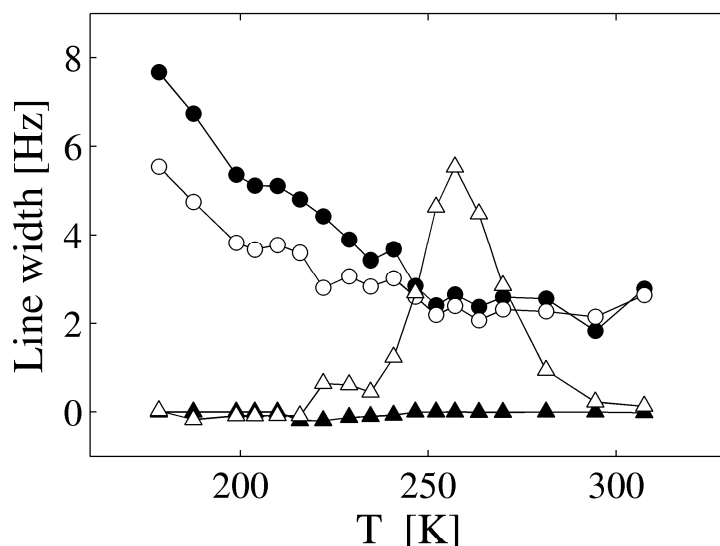


Figure S2. Line width contributions to hydride NMR spectra of complex **3** as a function of temperature. Circles: secular contribution; triangles: cross-relaxation contribution. Empty symbols: from fitting the central sub-spectrum; filled symbols: from fitting the  $^{195}\text{Pt}$  satellite. In both cases the 4-site model augmented with off-diagonal cross-relaxation terms has been employed.

The optimised secular and cross-relaxation width parameters for both central and satellite spectra are pictured in the Figure above. First, when cross-relaxation is not needed, its optimised value is very close to zero. Second, the secular line-width component of the central spectrum has temperature dependence quite similar to that of the satellite spectrum. Therefore, the cross-relaxation contribution does not mix with the secular line width and both width parameters are statistically uncorrelated.

Therefore, the additional broadening of the central transitions of the hydride NMR spectrum from molecules without  $^{195}\text{Pt}$ , which cannot be accounted for by an exchange phenomenon, can be rather explained by cross-relaxation between the transitions the frequency thereof does not depend on the  $^1\text{H}$ - $^{31}\text{P}$   $J$ -couplings. It however remains unclear which is the physical mechanism causing this additional relaxation and its relationship to the presence of  $^{195}\text{Pt}$  nuclei.

Supplementary material

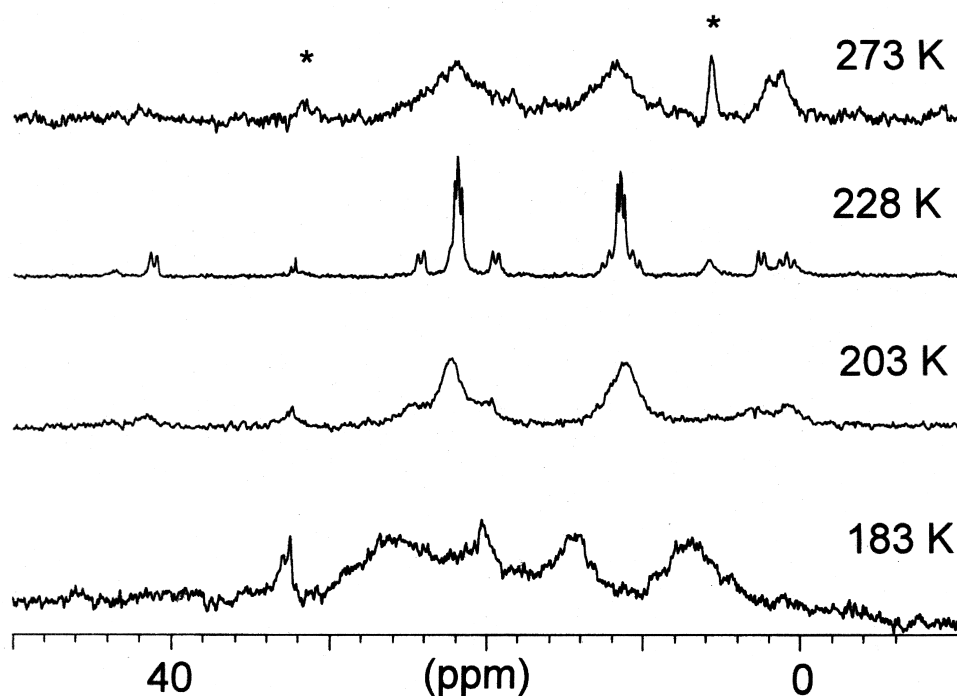


Figure S3. Selected  $^{31}\text{P}$  VT-NMR spectra for complex **3** in  $\text{CD}_2\text{Cl}_2$  at 121.49 MHz. \* denotes impurity. From top to bottom: at 273 K the broadening observed is due to the  $\text{P}_{cis}\text{-P}_{trans}$  exchange, at 228 K this motion is frozen and sharper signals appear, at lower temperature, 203 and 183 K, a further dynamic process becomes observable.

The figure above illustrates the dynamical behaviour of complex **3** in the temperature range 273-183 K. By lowering the temperature below 228 K (*i.e.* the freezing temperature for the  $\text{P}_{cis}\text{-P}_{trans}$  exchange) the onset of a further dynamic phenomenon is clearly evident. This process is still active at 183 K thus indicating a low activation energy dynamics. No further measurements at even lower temperature were possible because the sample solution freezes at 175 K.



### Supplementary material

$^{195}\text{Pt}$  Transition labelling with the  $^{31}\text{P}$  spin state configuration for complexes **1-3** in static (black) and dynamic (red) arrangements.

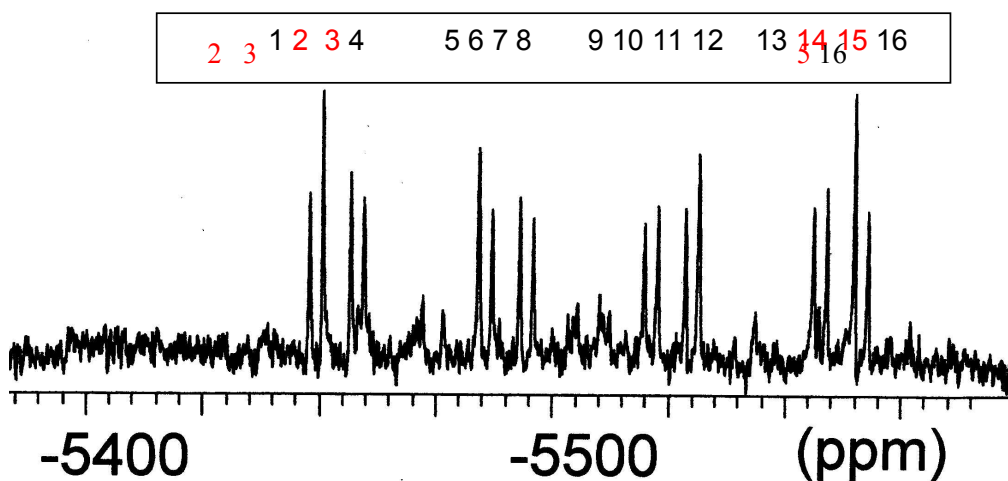


Figure S4.  $^{195}\text{Pt}$  spectrum of **1** at 300 K, 64.52 MHz. Red labels denote transitions unaffected by exchange dynamics.

Static spectrum:

1: $\beta\beta\beta\alpha$	2: $\beta\beta\beta\beta$	3: $\beta\beta\alpha\alpha$	4: $\beta\beta\alpha\beta$	5: $\beta\alpha\beta\alpha$	6: $\beta\alpha\beta\beta$
7: $\beta\alpha\alpha\alpha$	8: $\beta\alpha\alpha\beta$	9: $\alpha\beta\beta\alpha$	10: $\alpha\beta\beta\beta$	11: $\alpha\beta\alpha\alpha$	12: $\alpha\beta\alpha\beta$
13: $\alpha\alpha\beta\alpha$	14: $\alpha\alpha\beta\beta$	15: $\alpha\alpha\alpha\alpha$	16: $\alpha\alpha\alpha\beta$		

The fast-exchange spectrum is expected to consist of 9 transitions: a triplet of triplets centred at  $\delta_{\text{Pt}}$  with a large coupling  $J = (^1J_{\text{Pt-P1}} + ^1J_{\text{Pt-P3}})/2$  and a small one  $J = (^2J_{\text{Pt-P1}} + ^2J_{\text{Pt-P3}})/2$ , being transitions  $\beta\beta\beta\beta$  and  $\alpha\alpha\alpha\alpha$  the outermost lines.